

Effects of Variable Thermal Conductivity on Mhd Fluid Flow on Rotating Vertical Cone in the Presence of Darcy Forchheimer, Soret and Dufour Effects Through A Porous Medium

ABSTRACT

This research investigated the effects of Variable Thermal Conductivity on MHD fluid on a Rotating Vertical Cone in the Presence of Darcy Forchheimer, Soret and Dufour effects through a porous medium. The system of nonlinear differential equations were transformed into first order differential equations and solved using shooting technique in Matlab package Bvp4c. Furthermore, the effects of various parameters over the main physical quantities are shown graphically and also extensively discussed. The result shows that Thermal conductivity increases Tangential Velocity, Temperature and decreases Normal Velocity. Dufour increases Tangential Velocity and decreases Normal Velocity. Radiation parameter R enhances Tangential Velocity and Temperature.

Keywords: Darcy-Forchheimer, Soret, Dufour, Thermal Conductivity.

1. INTRODUCTION

The practical applications of thermal radiation in rotating fluid have increased greatly in the past decade. Simultaneous heat and mass transfer from different geometries embedded in porous media has many engineering and geophysical applications such as extraction of geothermal energy, drying of porous solids, food processing and storage, thermal insulation of buildings, enhanced oil recovery, nuclear power plants and cooling system of electronic devices.

In view of the above, unsteady mixed convection flow on a rotating cone in a rotating fluid, was studied by Anilkumar and Roy [1]. Unsteady heat and mass transfer from a rotating vertical cone with a magnetic field and heat generating or absorption effects, was analyzed by Chamkha and Ali [2]. It was established in the research that the tangential and azimuthal skin friction coefficients, local Nusselt and Shearwood numbers are linearly dependent with angular velocity of the cone. Ece [3], investigated free convection about a cone under mixed thermal boundary condition and magnetic field. Alim et al. [4], studied pressure work effect on natural convection flow from a vertical cone with suction and non-uniform surface temperature. Rotating disk flow and heat transfer of a conducting non-Newtonian fluid with suction injection and ohmic heating, was forwarded by Hazem and Attia [5]. Awad et al. [6], studied effects of convection from an inverted cone in a porous medium with cross diffusion. Cheng [7], studied natural convection boundary layer flow in a micro polar fluid over a vertical permeable cone with variable wall temperature. Kairi and Murthy [8] considered effects of viscous dissipation on natural convection heat and mass transfer from vertical cone in a non-Newtonian fluid saturated non-Darcy porous medium. Chamkha and Rashad [9], studied Natural convection from a vertical permeable cone in a nanofluid saturated porous media for uniform heat and nanoparticles volume fraction fluxes. El-Kabeir and El-Sayed [10] demonstrated effects of thermal radiation and viscous dissipation on MHD viscoelastic free convection past a vertical isothermal cone surface with chemical reaction. Kumar and Sivaraj [11], illustrated MHD viscoelastic fluid non-Darcy flow along a moving vertical cone. Natural convection of viscoelastic fluid from a cone embedded in a porous

medium with viscous dissipation was demonstrated by Gilvert et al. [12]. Malakarjuna et al [13], investigated the chemical reaction on MHD convective heat and mass transfer flow past a rotating cone embedded in a variable porosity regime. It was observed that an increase in the values of porosity and magnetic field parameter resulted in increase in the tangential skin-friction coefficient, local Nusselt and Sherwood numbers whereas the effects reverse significantly with azimuthal skin-friction coefficient. Dissipative slip flow along heat and mass transfer over a vertically rotating cone by way of chemical reaction with Dufour and Soret effects, was studied by Bilal et al. [14]. Sulochana et al. [15], illustrated similarity solution of 3D Casson non-Newtonian fluid flow over a stretching sheet with convective boundary condition. Pandit et al. [16], worked on effects of Hall current and rotation on unsteady MHD natural convection flow past a vertical flat plate with ramped wall temperature and heat absorption. Khan et al. [17], studied an improved heat conduction and mass diffusion models for rotating flow of an Oldroyd-B fluid. Magneto Jeffrey non-Newtonian bioconvection over a rotating vertical cone due to gyrotactic microorganism was demonstrated by Saleem et al. [18]. Interaction of micropolar fluid structure with the porous media in the flow due to rotating cone, was examined by Shahzad et al [19]. The study indicated that heat generated as a result of mass flux gradient, resulted in temperature profile enhancement, but opposite trend was the case in Prandtl number and micro rotation parameter. Magnetic field and porosity parameters adversely affected by increasing heat generated from the mass flux transfer.

For its frequent application in engineering and industries, the studies of fluid flow and heat transfer attracted the attention of many researchers. Cheng [20], investigated Soret and Dufour effects on natural convection boundary layer flow over a vertical cone in a porous medium with constant wall heat and mass fluxes. Soret and Dufour effects on viscoelastic boundary layer flow over a stretching surface with convective boundary condition with radiation and chemical reaction, argued by Eswaramoorthi et al., [21]. In the results of the study, it was observed that the velocity and its boundary layer thickness decrease as the unsteadiness parameter increases. This exhibits the growth of change of laminar flow to turbulent flow. The study clearly shows that the thermal diffusion effect slightly affects the fluid concentration, as the values of Soret number increases. It was also noticed that the diffusion thermal effects greatly affect the fluid temperature, an increase in Dufour number corresponds to an increase in the fluid temperature and the thermal boundary layer thickness. Numerical investigation of magnetohydrodynamic (MHD) radiative flow over a rotating cone in the presence of Soret and chemical reaction, was analysed by Sulonocha et al., [22]. It was found that magnetic field parameter has tendency to control the momentum boundary layer. Porosity and buoyancy parameter are capable of enhancing convection in the fluid flow. Krishnandan et al [23] studied Soret and Dufour effects on MHD flow about a rotating vertical cone in the presence of radiation.

A controlled fluid flow plays a significant role in industries and agricultural activities. Therefore, the physical application of Darcy-Forchheimer cannot be overemphasized. Hayat et al., [24] investigated the Forchheimer flow with variable thermal conductivity and Cattaneo-Christov heat flux. Darcy-Forchheimer flow due to a curved stretching surface with Cattaneo-Christov double diffusion was presented by Hayat et al., [25]. Upreti et al. [26] perceived ohmic heating and non-uniform heat source/sink roles on 3D Darcy-Forchheimer flow of CNTs nanofluid over a stretching surface. Irreversibility analysis in Darcy-Forchheimer flow of viscous fluid with Dufour and Soret effects via finite difference method, was forwarded by Sohail et al. [27]. Loganathan et al. [28] investigated the significance of Darcy-Forchheimer porous medium in third grade nanofluid with entropy features. Analytical and numerical investigation of Darcy-Forchheimer flow of a nonlinear radiative non-Newtonian fluid over a Riga plate with entropy optimization, was done by Eswaramoorthi et al., [29].

Chebyshev finite difference method for the effects of variable viscosity and variable thermal conductivity on heat transfer from surfaces with radiation was studied by Elsayed and Nasser, [30]. Two cases were considered, one corresponding to a plane surface moving in a

parallel with free stream while the other, a surface moving in the opposite direction to the free stream. The results indicated that variable viscosity, variable thermal conductivity, radiation and permeability have significant influences on the velocity, the angular velocity and the temperature profiles, Sherwood stress, couple stress and Nusselt number in both cases. There after many studies were conducted on effects of variable viscosity and thermal conductivity under different physical conditions and variable fluid properties by [31-36].

Muhammad and Sarah [37], presented a new type of shooting method for non-linear boundary value problems. It concluded that enhanced method of shooting technique is more accurate and applicable than built in method used in different software packages. Shooting method in solving boundary value problems was studied by Badrdeen and Mohsin [38]. Summiya [39], studied numerical solution of the Falkner Skan equation by using shooting techniques. Chang [40] illustrated Numerical solution of Troesch's problem by simple shooting method.

From the above literature, it was observed that the effects of Thermal Conductivity, Thermo-diffusion, Diffusion-thermo, second order porous resistance (Forchheimer) on MHD fluid flow in a rotating vertical cone has not been adequately investigated. The objective of this research is to fill the gap on the work of Sulonocha et al., [22]. Therefore, this research focused on the investigation effects of variable thermal conductivity on MHD fluid on a rotating vertical cone in the presence of Darcy-Forchheimer, Soret and Dufour effects. Furthermore, the effects of various parameters over the main physical quantities are presented graphically and also extensively discussed. The problem is solved numerically using inbuilt Runge Kutta shooting technique in Matlab package Bvp4c.

2. MATERIAL AND METHODS

Consider a steady two-dimensional, incompressible, electrically conducting boundary layer flow induced by a rotating vertical cone with an angular velocity Ω embedded in a variable porosity medium as shown in Figure 1. A uniform magnetic field is applied in z-direction normal to the cone surface. It is assumed that the fluid properties are to be isotropic and constant except the density variation in the buoyancy force term of the momentum equations. Induced magnetic field is neglected in this study. In addition, it is also assumed that the first order homogeneous chemical reaction along with thermal radiation, Soret, Dufour, Darcy Forchheimer and heat generation/ absorption are taken into account. The variable thermal conductivity k_c is assumed to vary as linear function of temperature in the

form given by Elsayed and Nasser, [30]. $k_c = k_0 \{1 + m^* (T - T_\infty)\}$, where k_0 is the thermal conductivity of the ambient fluid and m^* is the constant depending of the nature of the fluid.

Where $m^* > 0$ for fluid such as water and air, while $m^* < 0$ for fluid such as lubricants, Elsayed and Nasser, [30]. This form can also be expressed as;

$k_c = k_0(1 + Q\theta)$, where $Q = m^* (T - T_\infty)$, is the thermal conductivity parameter and T is the value of temperature of the cone.

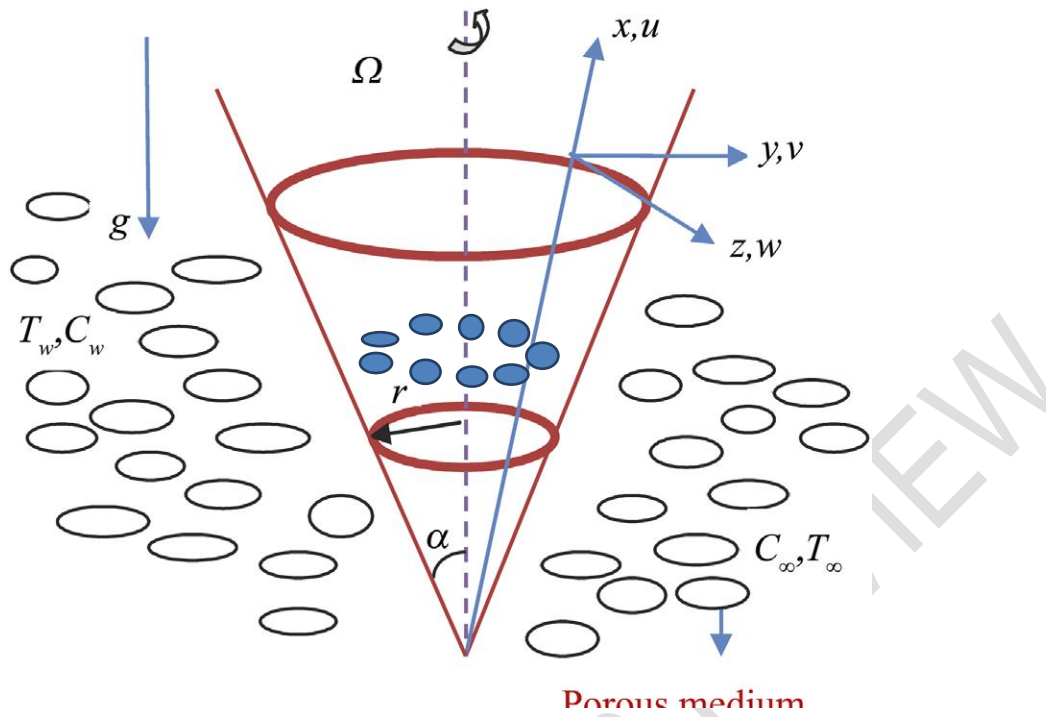


Figure 1. Schematic diagram of the model.

Under the above conditions, the governing boundary layer equations are for Continuity, Momentum in U direction, Momentum in V direction, Energy and Mass transfer, given as Sulonocha et al., [22].

The Mass Continuity Equation;

$$\frac{\partial u}{\partial x} + \frac{\partial u}{\partial z} + \frac{u}{x} = 0 \quad (1)$$

The U-direction Momentum Equation.

$$-\varepsilon^{-2} \rho \left(u \frac{\partial u}{\partial x} + w \frac{\partial u}{\partial z} - \frac{v^2}{x} \right) = \varepsilon^{-1} \mu \frac{\partial^2 u}{\partial z^2} + \rho g (\beta_T (T - T_\infty) + \beta_C (C - C_\infty)) \cos \alpha - \sigma B_0^2 u - \frac{\mu u}{K} + \frac{F}{\sqrt{K}} u^2 \quad (2)$$

The V-direction Momentum Equation.

$$\varepsilon^{-2} \rho \left(u \frac{\partial u}{\partial x} + w \frac{\partial u}{\partial z} - \frac{uv}{x} \right) = \varepsilon^{-1} \mu \frac{\partial^2 v}{\partial z^2} - \sigma B_0^2 u - \frac{\mu}{K} v + \frac{F}{\sqrt{K}} v^2$$

(3)

The Energy Equation;

$$u \frac{\partial T}{\partial x} + w \frac{\partial T}{\partial z} = \frac{k_0}{\rho c_p} \frac{\partial}{\partial z} \left[(1 + m^* (T - T_\infty)) \frac{\partial T}{\partial z} \right] - \frac{Q}{\rho c_p} (T - T_\infty) - \frac{1}{\rho c_p} \frac{\partial q_r}{\partial z} + \frac{D_m K_r \partial^2 C}{C_s \partial z^2} \quad (4)$$

The Mass Concentration Equation.

$$u \frac{\partial C}{\partial x} + w \frac{\partial C}{\partial z} = D \frac{\partial^2 C}{\partial z^2} - K_r (C - C_\infty) + \frac{D_m k_T \partial^2 T}{T_m \partial z^2} \quad (5)$$

With the following boundary conditions;

$$\left. \begin{aligned} u = 0, \quad v = r\Omega, \quad w = 0, \quad T = T_w(x), \quad C = C_w(x), \quad \text{at } z = 0 \\ u = 0, \quad v = 0, \quad T = T_\infty, \quad C = C_\infty, \quad \text{as } z \rightarrow \infty \end{aligned} \right\} (6)$$

where x-axis is along a meridional section, y-axis is along a circular section and the z-axis is normal to the cone surface, u, v and w are the velocity components along the tangential (x), circumferential or azimuthal (y) and normal (z) directions respectively, r is radius of the cone, Ω is the angular velocity of the rotation. ε is the porosity parameter, ρ is the fluid density, μ is the dynamic viscosity, c_p specific heat at constant pressure, g is the acceleration due to gravity, β_T and β_C are the thermal and concentration coefficients, α is the cone apex half angle, K is the permeability of the porous medium, k_0 is the effective thermal conductivity, K_r is the chemical reaction parameter and D is the molecular diffusivity. The porous medium parameter F_n may become similarity parameter if the non-uniform inertial

coefficient of porous medium is defined as $F = \frac{C_d}{x}$ where C_d is drag coefficient. In this

case the expression for $Fu = \frac{C_d}{\sqrt{K}}$ is a similarity parameter since it is independent of x . [25-

26]

In order to obtain non-dimensional equations, we introduce the radiation parameter in dimensional form as;

$$qr = - \left(\frac{4\sigma_0}{3k} \right) \frac{\partial T^4}{\partial y} \quad (7)$$

Where σ_0 is the Stefan-Boltzmann constant and k is the absorption coefficient. Assuming the difference in temperature within the flow is such that T^4 can be expressed as a linear combination of temperature, we expand the T^4 in Taylor's series about T_∞ as follows;

$$T^4 = T_\infty^4 + 4T_\infty^3(T - T_\infty) + 6T_\infty^2(T - T_\infty)^2 + \dots (8)$$

Neglecting higher order terms beyond the first degree in $(T - T_\infty)$ we have

$$T^4 = -3T_\infty^4 + 4T_\infty^3 T (9)$$

Differentiating (7) with respect to y and using (9), equation (7) transformed to;

$$\frac{\partial qr}{\partial z} = -\frac{16T_\infty^3 \sigma}{3k} \frac{\partial^2 T}{\partial z^2} (10)$$

As defined by (Eswaramoorthi et al., 2016).

The above equations (1)-(6) representing the governing equations of the fluid flow and the boundary conditions in dimensioned form. Equations (1)-(6) can be transformed to dimensionless form by introducing the non-dimensional quantities below to obtain the solutions in similarity form.

$$\left. \begin{aligned} \eta &= \left(\frac{\Omega \sin \alpha}{\nu} \right)^{1/2} z, \quad u = x \Omega \sin \alpha f(\eta), \quad v = x \Omega \sin \alpha g(\eta), \quad r = x \sin \alpha, \quad w = (\nu \Omega \sin \alpha)^{1/2} h(\eta) \\ \theta(\eta) &= \frac{T - T_\infty}{T_w - T_\infty}, \quad \phi(\eta) = \frac{C - C_\infty}{C_w - C_\infty}, \quad T_w(x) - T_\infty = \frac{(T_L - T_\infty)x}{L_n}, \quad C_w(x) - C_\infty = \frac{(C_L - C_\infty)x}{L_n} \\ Da^{-1} &= \frac{\nu}{K \Omega \sin \alpha}, \quad M = \frac{Ha^2}{R_{eL}}, \quad Ha^2 = \frac{\sigma B_0^2 L_n^2}{\mu}, \quad R_{eL} = \frac{\Omega L^2 \sin \alpha}{\nu}, \quad \lambda = \frac{Gr_L}{R_{eL}^2} \\ Gr_L &= \frac{g_s \beta_T \cos \alpha (T_w - T_\infty) L_n^2}{\nu^2}, \quad N = \frac{\beta_C (C_w - C_\infty)}{\beta_T (T_w - T_\infty)}, \quad Pr = \frac{k_0}{\mu C_p}, \quad Sc = \frac{\nu}{D}, \quad \gamma = \frac{K_r}{\Omega \sin \alpha} \\ Sr &= \frac{D_m D_T}{\nu T_\infty} \left(\frac{T_L - T_\infty}{C_L - C_\infty} \right), \quad R = \frac{4\sigma T_\infty^3}{\rho C_p K^* k_0}, \quad F_u = \frac{FVx}{\mu \sqrt{K}}, \quad Q = m(T - T_\infty) \end{aligned} \right\} (11).$$

Where L_n being the cone slant height and T being the cone surface temperature and C being the cone surface concentration at the base ($x=L_n$).

s

$$f = -\frac{1}{2} h' (12)$$

$$\varepsilon^{-1} h''' - 2\lambda(\theta + N\phi) + \varepsilon^{-2} \left(\frac{1}{2} h'^2 - hh'' - 2g^2 \right) - (M + Da^{-1})h' - \frac{1}{2} F_u h'^2 = 0 (13)$$

$$\varepsilon^{-1} g'' - \varepsilon^{-2} (h'g + hg') - (M + Da^{-1})g - F_u g^2 = 0 (14)$$

$$\left(\frac{(1+Q\theta)+R}{Pr}\right)\theta''-h\theta'-Qh\theta+\frac{1}{2}h'\theta+Df\phi''+\frac{1}{Pr}Q(\theta')^2=0 \quad (15)$$

$$\frac{1}{Sc}\phi''-\gamma\phi+Sr\theta''+\frac{1}{2}h'\phi-h\phi'=0 \quad (16)$$

The corresponding initial and boundary conditions are;

$$\left. \begin{aligned} f=h'=0, \quad g=1, \quad \theta=1, \quad \phi=1 & \quad \text{at } \eta=0 \\ h'=0, \quad g=0, \quad \theta=0, \quad \phi=0 & \quad \text{as } \eta \rightarrow \infty \end{aligned} \right\} (17)$$

Where the primes denote differentiation with respect to η . Here is the transformed coordinates of f, g and h which are dimensionless velocity components along the tangential, azimuthal and normal directions respectively. θ is the dimensionless temperature, ϕ is the dimensionless concentration. Da^{-1} is the inverse of Darcy number, Gr_L Grashof number Re_L is the Reynold number λ is the dimensionless buoyancy parameter, N is the buoyancy ratio, M is the dimensionless magnetic parameter, Ha^2 is the Hartmann number Sc is the Schmidt number, R is the Radiation parameter Sr is the Soret parameter, Df is the Dufor parameter, μ coefficient of viscosity F_u is the Darcy-Forchheimer (second order porous resistance) parameter.

It is part of fundamentals of this research to find the parameters of physical interest in fluid flow, heat and mass transfer. The result on local surface skin frictions coefficient in x and y directions, local Nusselt number and local Sherwood number are given in dimensionless form as follows;

$$Cf_x Re^{\frac{1}{2}} = -h''(0) \quad 2^{-1} Cf_y Re^{\frac{1}{2}} = -g'(0) \quad Re^{\frac{1}{2}} Nu_x = -\theta'(0) \quad Re^{\frac{1}{2}} Sh_x = -\phi'(0)$$

2.1 Numerical Procedure. The equations (8)-(13) represent the dimensionless governing equations and the dimensionless boundary conditions. The system of linear ordinary differential equation is converted to first order ordinary differential equation and solved numerically using bvp4c Matlab package Uwanta et al [42] and Sulonocha et al., [22]. Consider the following assumptions;

$$\left. \begin{aligned} h = y_1 \quad h' = y_2 \quad h'' = y_3 \quad g = y_4 \quad g' = y_5 \quad \theta = y_6 \quad \theta' = y_7 \\ \phi = y_8 \quad \phi' = y_9 \end{aligned} \right\} (18)$$

The system of nonlinear differential equations is then transformed into the following first order differential equations as follows;

$$\begin{aligned}
y_1' &= -2y_2 \\
y_2' &= y_2 \\
y_3' &= -\varepsilon \left[\varepsilon^{-2}y_1y_3 + (M + Da^{-1})y_2 + \varepsilon^{-2}\left(-\frac{1}{2}y_2^2 + 2y_4^2\right) - \right. \\
&\quad \left. 2\lambda(y_6 + Ny_8) + \frac{1}{2}F_u y_2^2 \right] \\
y_4' &= y_5 \\
y_5' &= \varepsilon \left[\varepsilon^{-2}(y_1y_2 - y_2y_4) + (M + Da^{-1})y_4 + F_u y_4^2 \right] \\
y_6' &= y_7 \\
y_7' &= \frac{3Pr}{(3(1+Qy_6) + 4R)} \left[y_1y_7 - \frac{1}{2}y_2y_6 + Q_H y_6 - \frac{1}{Pr}Q(y_7)^2 - D_f y_9' \right] \\
y_8' &= y_9 \\
y_9' &= -Sc \left[Sr(y_7') + \frac{1}{2}y_2y_8 - y_1y_9 - \gamma y_8 \right]
\end{aligned} \tag{19}$$

3. RESULTS AND DISCUSSION

The numerical results reporting the influence of radiation, porosity, thermal conductivity, Dufour, buoyancy and second order porous medium (Forchheimer).

The default values for the parameters are;

$$\varepsilon = 2, M = 0.01, \lambda = 5, D = N = R = Sr = Df = \gamma = 1$$

$$Pr = 0.6, Qh = 0.5, Sc = 0.6, F_u = 0.2, Q = 0.2.$$

Figures 2-4 depicted effects of radiation parameter (R) on temperature, normal and tangential velocities. Increase in R leads to generation of heat to the fluid and make boundary layer to be thinner which result to easy flow of the fluid and rises temperature of the fluid. From the figure it is clearly observed that due to influence of radiation parameter, the tangential velocity and the temperature increase with increase in R, while normal velocity decreases.

Figures 5-7 described the distribution of porosity parameter (ε) on velocity and temperature. The figures indicated that a decrease in normal velocity is attained as the porosity parameter (ε) increases and the reverse is the case in tangential velocity and temperature profiles.

Figures 8-10 depicted velocity and temperature profiles on thermal conductivity parameter (Q). Decrease in normal velocity as the value of the thermal conductivity increases, but the opposite trend is observed in case of tangential and temperature profiles. This means the thermal conductivity energises the boundary layer thereby increasing the tangential velocity and temperature of the fluid.

The display in figures 11-14 portray the influence of Dufour (Df) effects on temperature and velocity profiles. It was observed that Concentration and Normal velocity increase with increase in Df, while Tangential velocity and temperature decrease with increasing Df.

Figures 15-18 demonstrated the effects of buoyancy parameter on velocity, temperature and concentration profiles. Rise in buoyancy parameter enhances tangential velocity and on the other hand normal velocity, temperature and concentration have quite opposite effects. Figures 19-22 depicted the effects of second order porous medium on normal, tangential velocities, temperature and concentration on fluid flow. Figure 22 indicates the influence of second order porous medium effects on Normal velocity, it is noted that increase in the values of F_u decrease the normal velocity of the fluid. In figure 23, the escalated values of F_u resulted to increase in the Tangential velocity of the fluid, this indicates that F_u is linearly dependent on Tangential velocity. Decrease in mass transfer is expected as the thermal boundary layer become thicker as the temperature of the fluid reduced. This can be witnessed from figures 23 and 24 the effects of F_u on temperature and concentration of the fluid flow respectively.

Table 1. Comparison of surface shear stresses ($-h'(0)$) and surface heat transfer $-\theta'(0)$ with previous results on a scale of $M=R=N=Qh=F_u=Df=Sc=Sr=0$

	Δ Present results (Sulochana et al, 2018)		(Mallikarjuna et al, 2015)			
	$-h''(0)$	$-\theta''(0)$	$-h''(0)$	$-\theta''(0)$	$-h''(0)$	$-\theta''(0)$
0	0.6158	0.4304	0.6158	0.4284	0.6158	0.4284
0.1	0.6544	0.4619	0.6549	0.4614	0.6549	0.4614
1	0.8507	0.6120	0.8508	0.6121	0.8508	0.5121
10	1.4037	1.0173	1.4036	1.0176	0.4037	1.0175

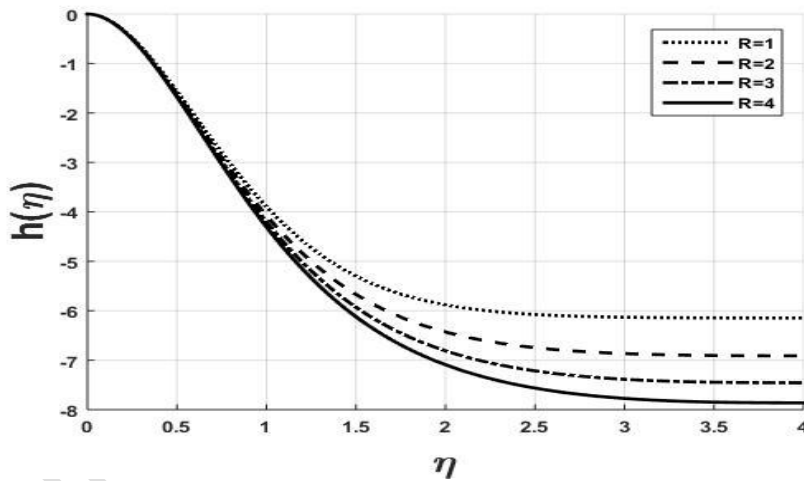


Fig. 2 Normal Velocity distribution on radiation parameter (R)

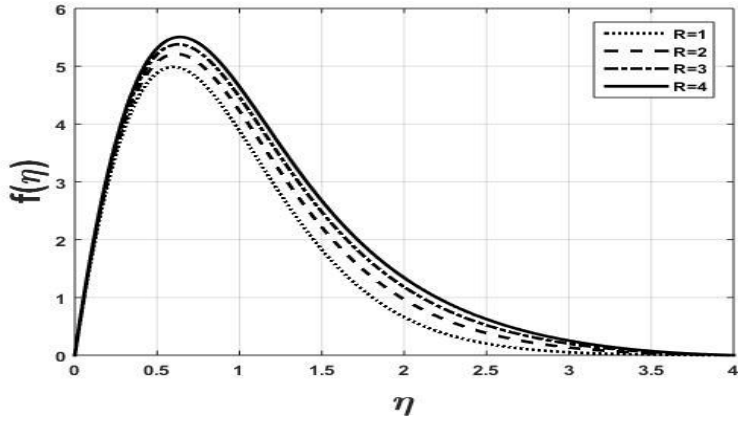


Fig. 3 Tangential Velocity distribution on radiation parameter (R)

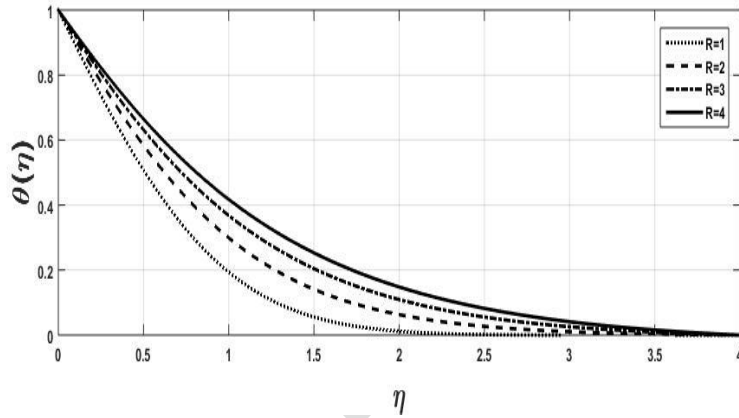


Fig 4. Temperature distribution on Radiation (R)

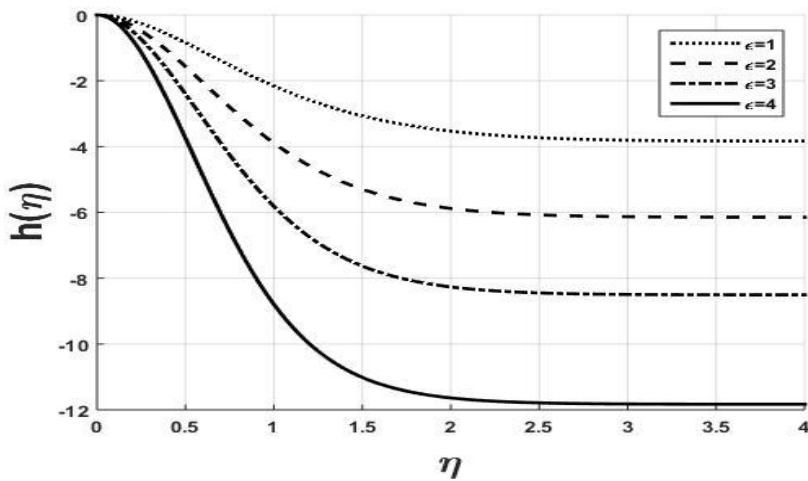


Fig. 5 Normal velocity distribution on Porosity(ϵ).

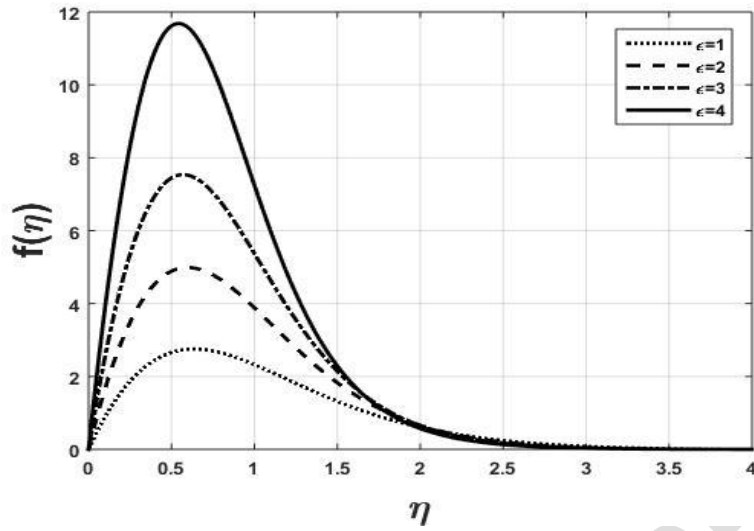


Fig.6 Tangential velocity distribution on Porosity (ϵ)

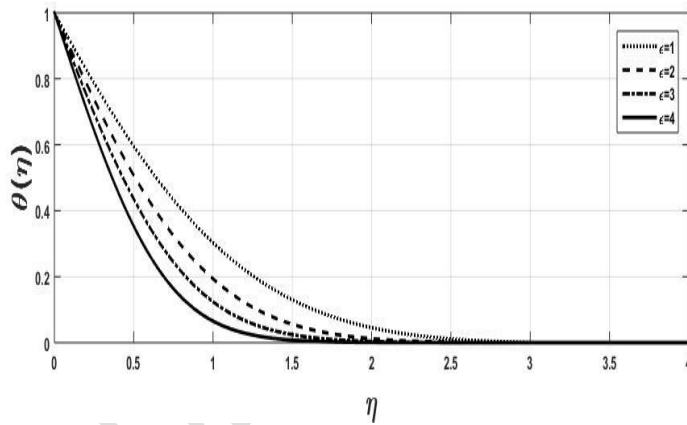


Fig.7 Temperature distribution on Porosity (ϵ).

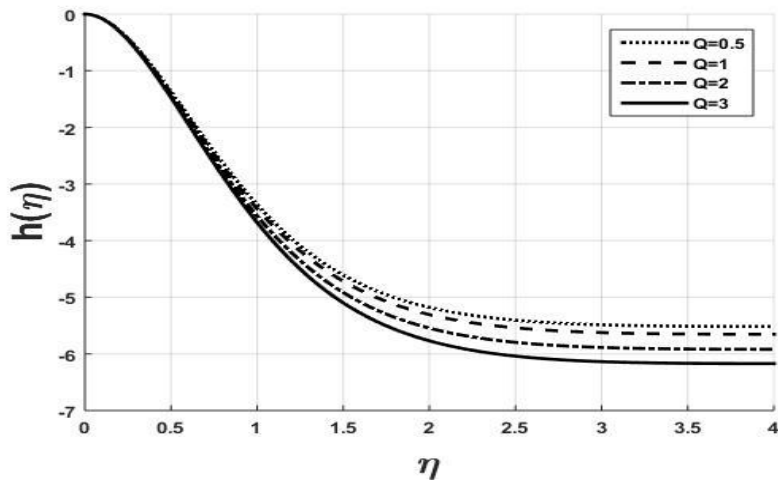


Fig.8 Normal Velocity distribution due to thermal conductivity parameter (Q)

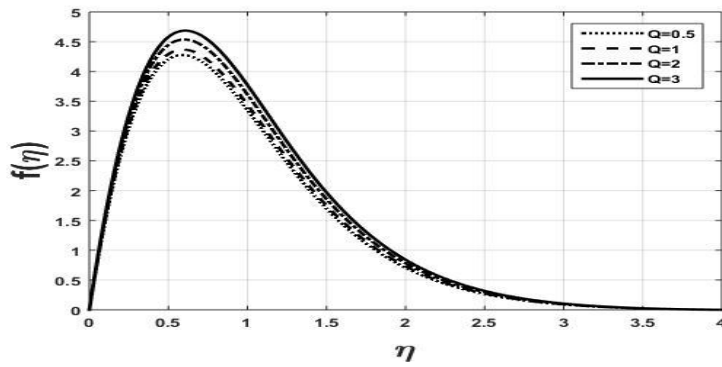


Fig.9. Tangential Velocity distribution due to thermal conductivity parameter (Q)

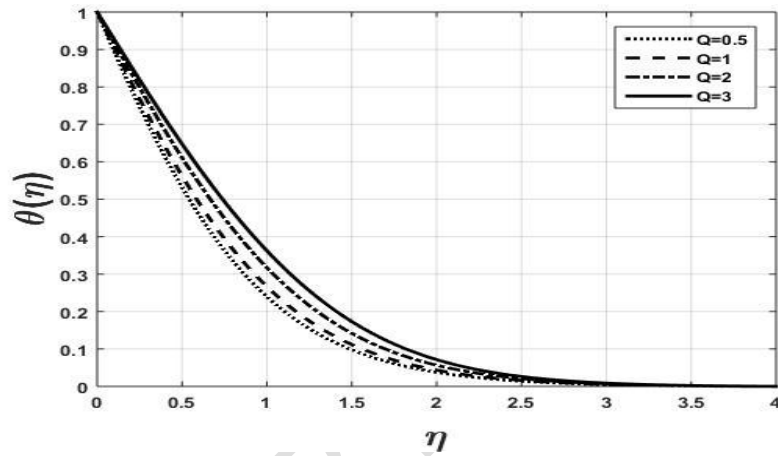


Fig.10 Temperature distribution due to thermal conductivity parameter (Q)

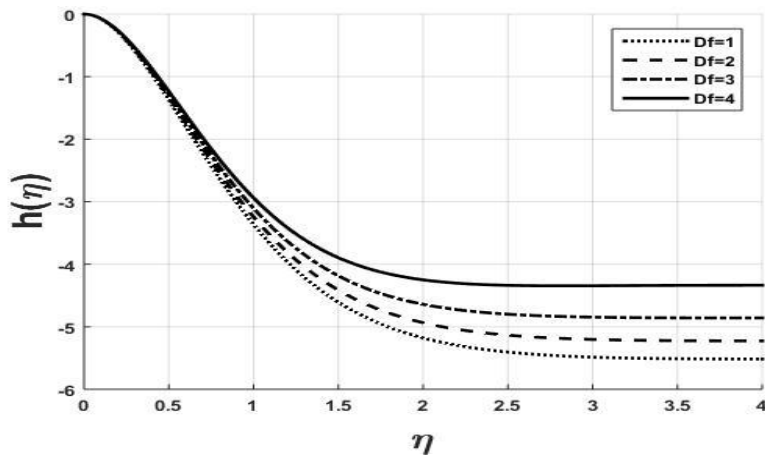


Fig.11 Normal Velocity distribution on Dufor (Df)

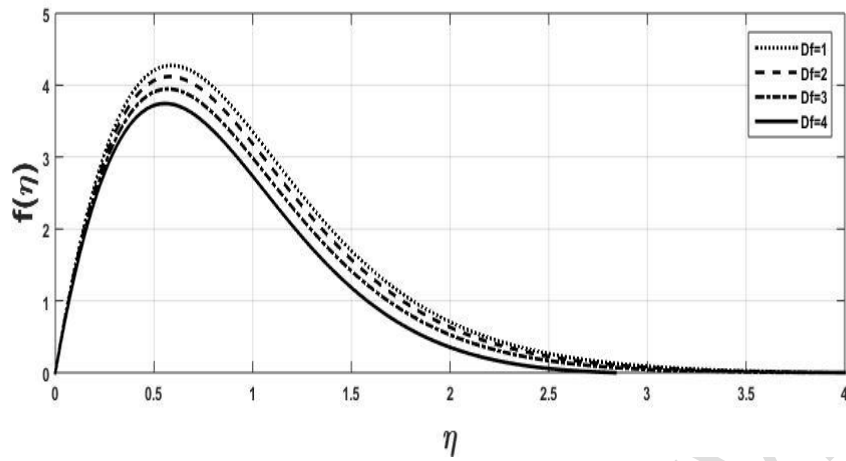


Fig. 12 Tangential Velocity distribution due to Dufor (Df) variation

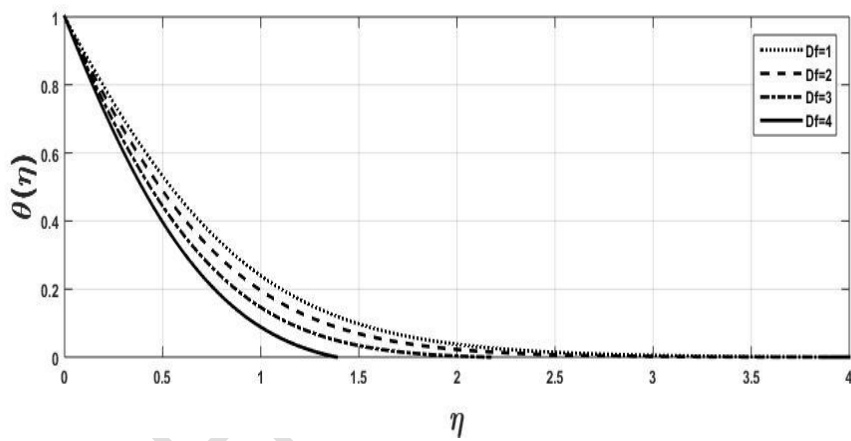


Fig. 13 Temperature distribution due to Dufor (Df) variation.

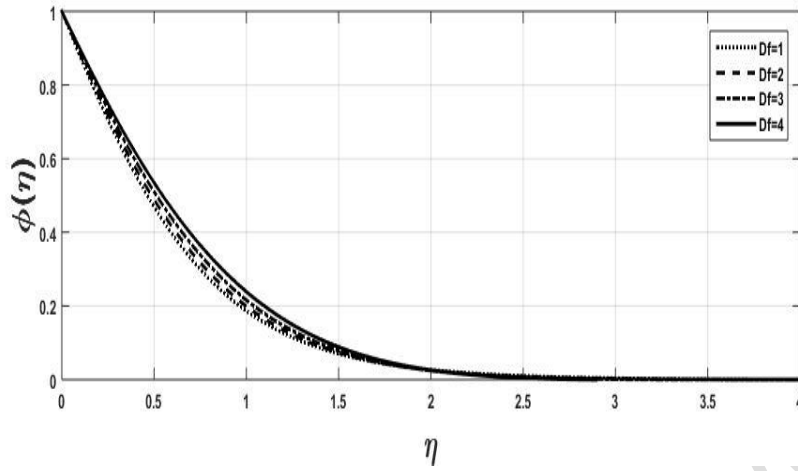


Fig. 14 Concentration distribution on Dufor(Df)

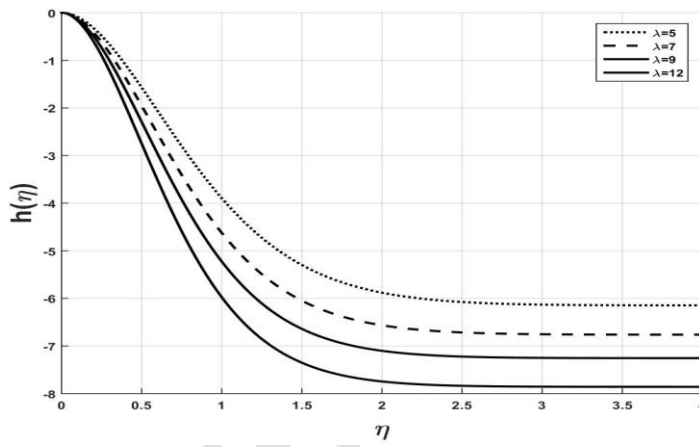


Fig. 15 Normal Velocity distribution on buoyancy parameter (λ)

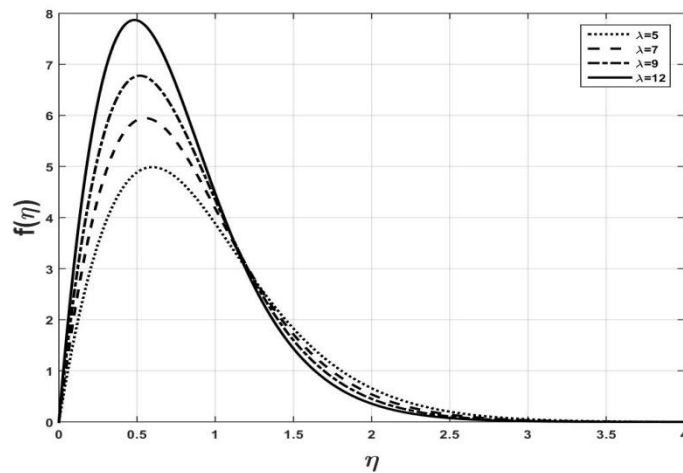


Fig. 16 Tangential Velocity on buoyancy parameter (λ)

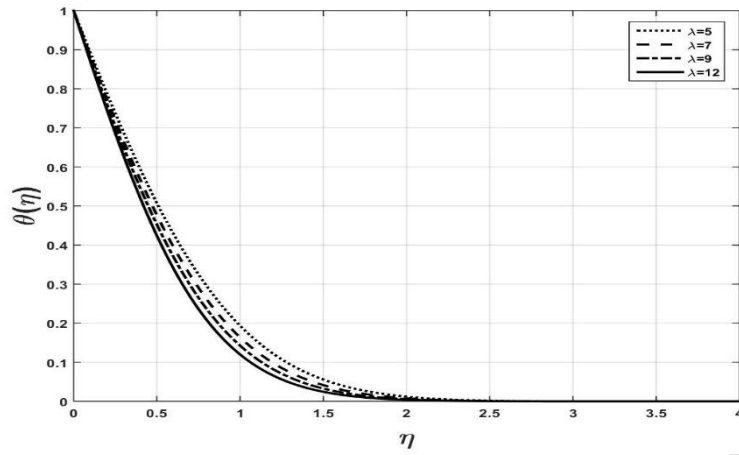


Fig. 17 Temperature distribution on buoyancy parameter (λ)

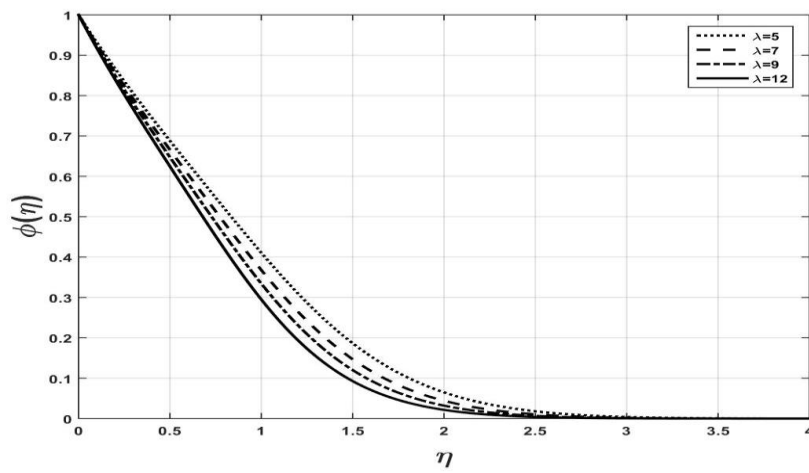


Fig. 18 Concentration distribution on buoyancy parameter (λ)

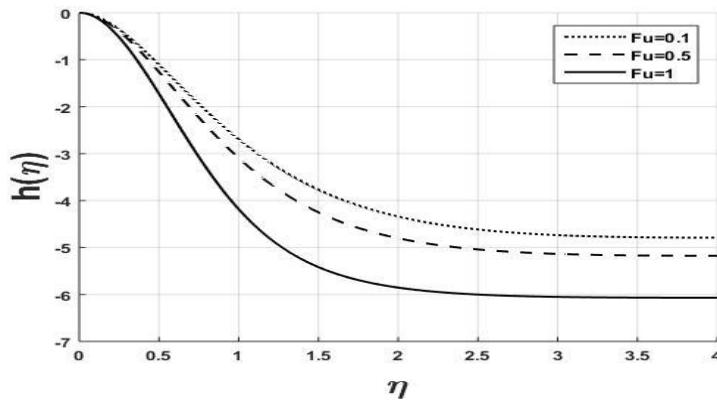


Fig. 19 Normal Velocity distribution on Darcy-Forchheimer (F_u)

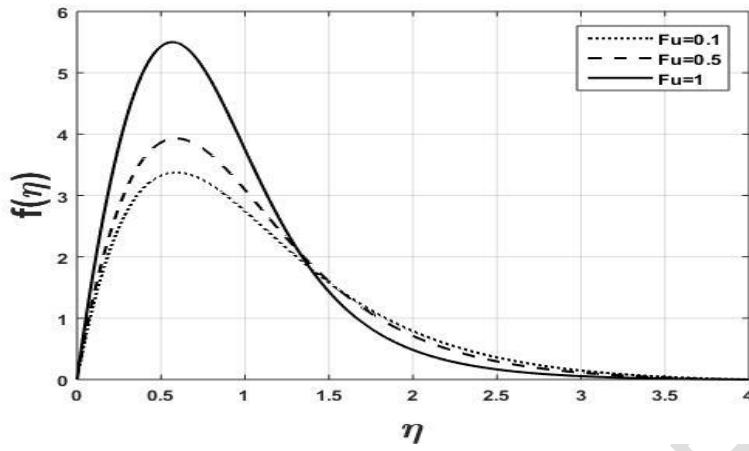


Fig. 20 Tangential Velocity distribution on Darcy-Forchheimer (F_u)

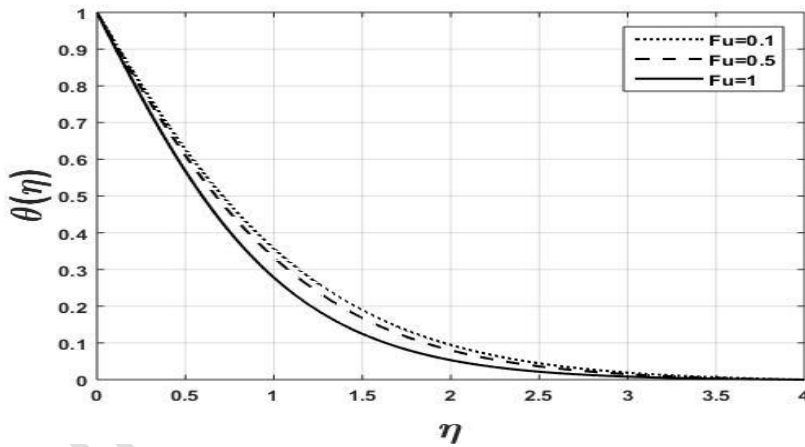


Fig. 21 Temperature distribution on Darcy-Forchheimer (F_u)

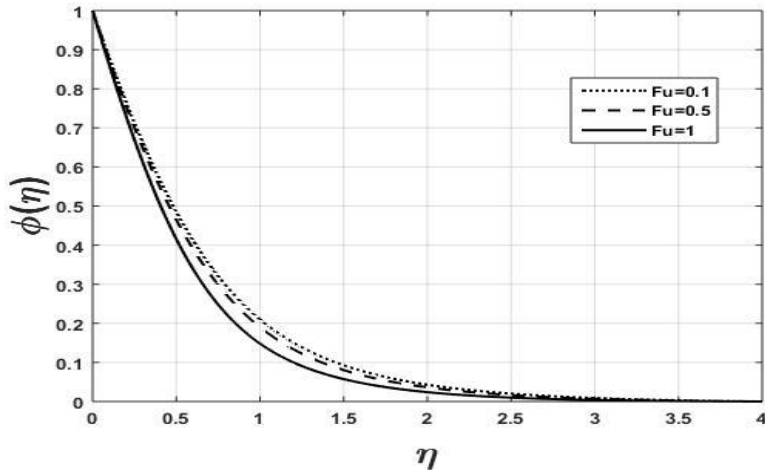


Fig. 22 Concentration distribution on Darcy-Forchheimer (F_u)

Table 2: indicated numerical values of Skin frictions along tangential and circumferential directions, Nusselt number and Sherwood number for different values of some selected parameters. It is observed that increase in porosity (ε) and Forchheimer (L) parameters increases friction along tangential and circumferential directions and rate of heat and mass transfer. It is also clear that increase in the values of Dufor (D_f) parameter decrease frictions and mass transfer but increases the rate of heat transfer, this is because of the heat generated from massflux transfer. Increasing values of Soret and Variable Thermal conductivity parameter enhanced frictions as a result of increase in massflux transfer generated from temperature gradient (thermal diffusion).

Table 2. Variation in Friction factors, local Nusselt numbers and local Shearwood numbers

ε	RQL	D_f	S_r	$-h''(0)$	$-g'(0)$	$-\theta'(0)$	$-\phi'(0)$
1				10.012926	1.596751	0.876727	0.561270
2				18.706899	1.594001	1.080060	0.704153
3				28.500804	1.648224	1.256705	0.844244
4				42.992169	1.777830	1.473158	1.029433
	1			18.706899	1.594001	1.080060	0.704153
	2			19.066298	1.613416	0.915966	0.904346
	3			19.332637	1.626958	0.808346	1.035224
	4			19.537987	1.637006	0.731928	1.127096
.5				16.893788	1.516471	1.057771	1.263705
1	17.107112	1.526741		0.957236	1.314479		
2				17.478601	1.544670	0.819422	1.382332
3				17.795234	1.559908	0.727746	1.426446
.2				16.893788	1.516471	1.057772	1.263705
.4				18.158856	1.642325	1.092714	1.305315
.6				20.087986	1.779840	1.140876	1.362688
.8				23.504044	1.946405	1.214631	1.453314
1				16.893788	1.516471	1.057770	1.263705
2				16.554138	1.499095	1.198241	1.190213
3				16.180457	1.478808	1.334544	1.116928

4	15.753206	1.453575	1.465788	1.042127
1	16.893788	1.516471	0.057991	1.263705
2	17.512957	1.544039	1.066538	1.068244
3	18.117349	1.569812	1.074087	0.881720

REFERENCES

- [1] Anilkumar, D, Roy, S. Unsteady mixed convection flow on a rotating cone in a rotating fluid. *Applied Mathematics and Computation*. (2004): 155, 545-561.
- [2] Chamkha, AJ, Ali, A. Unsteady heat and mass transfer from a rotating vertical cone with a magnetic field and heat generation or absorption effects. *International Journal of Thermal Science*. (2005): 44, 267-276.
- [3] Ece, CM. Free convection about a cone under mixed thermal boundary conditions and a magnetic field. *Applied Mathematical Modelling*. (2005): 29, 1121-1134..
- [4] Alim, MA, Alam, M Md, Chowdhury, MK. Pressure work effectson natural convection flow from a vertical circular cone with suction and non-uniform surface temperature. *Journal of Mechanical Engineering*. (2006):36, 6-11.
- [5] Hazem, AA. Rotating disk flow and heat transfer of a conducting non newtonian fluid with suction injection and ohmic heating. *Journal of the Braz. Soc. of Mech. Sci. and Eng. Xxix*, (2007):2 168-173.
- [6] Award, FG, Sibanda, P. Motsa, SS, Makinde OD. Convection from an inverted cone in a porous medium with cross diffusion effects. *Computer and Mathematics with application*. (2011): 61, 1431-1441
- [7] Cheng, CY. Natural convection boundary layer flow in a micropolar fluid over a vertical permeable cone with variable wall temperature. *International Communications in Heat and Mass Transfer*. (2011b) 38, 429-433.
- [8] Kairi, RR, Murthy, PVS. Effect of viscous dissipation on natural convection, heat and mass transfer from vertical cone in a non-Newtonian fluid saturated non-Darcy porous medium. *Applied Mathematics and Computation*. (2011):217, 8100-8114.
- [9] Chamkha, AJ, Rashad, AM. Natural convection from a vertical permeable cone in a nano fluid saturated porous media for uniform heat and nano particles volume fraction fluxes. *International Journal of Numerical Methods for Heat & Fluid Flow*. (2012): 22, 1073-1085.
- [10] El-Kabeir, SM, El-Sayed, EA. Effects of thermal radiation and viscous dissipation on mhd viscoelastic free convection past a vertical isothermal cone surface with chemical reaction. *International Journal of Energy and Technology*. (2012):4, 1-7 (2012)
- [11] Kumar, M, Sivaraj, R. MHD viscoelastic fluid non-Darcy flow along a moving vertical cone. *International Journal of Applied Mathematics and Mechanics*. (2012): 8, 69-81
- [12] Gilvert, M, Makinde OD. Precious S. Natural convection of viscoelastic fluid from a cone embedded in porous medium with viscous dissipation. *Hindawi Mathematical problems in Engineering* volume 2013. Article ID 934712, 1- 11,

- [13] Malikarjuna, B, Rashed, AM, Chamkha AJ. Chemical reaction on MHD convective heat and mass transfer flow past a rotating cone embedded in a variable porosity regime. *African Mathematical Union*. 1-22 (2015) DOI10.1007/s13370-015-0372-1
- [14] Bilal, S, Khalil, UR, Raman, HJ, Malik, MY, Salahuddin, T: Dissipative slip flow along heat and mass transfer over a vertically rotating cone by way of chemical reaction with dufor and soret effects. *API Advances*. (2016): 6, 125-135.doi.org/10.1063/1.4973307
- [15] Sulonocha, C, Ashwinkumar, GP, Sandeep N. Similarity solution of 3d cassonnona fluid flow over a stretching sheet with convective boundary condition. *Journal of Nigerian Mathematical Society*. (2016): 35, 128-141.
- [16] Pandit, KK, Sarma, D, Deka AK. Effects of hall current and rotation on unsteady MHD natural convection flow past a vertical flat plate with ramped wall temperature and heat absorption. *British Journal of Mathematics and Computer Science*. (2016): 18(5), 1-26 Article no.BJMCS 27221.
- [17] Khan, WA, Irfan, M, Khan, M. An improved heat conduction and mass diffusion models for rotating flow of an old royd-b fluid. *Result in Physics*. (2017): 7, 3583-3589.
- [18] Saleem, S, Hunza, R, Al-Qahtani, A, Abd-El-Aziz M, Malik MY, Animasaun, IL. Magneto jeffreynonafluid bioconvection over a rotating vertical cone due to gyrotatic microorganism. *Mathematical problems in Engineering. Hindawi*, 2019, Art. ID 3478037, 11pp.
- [19] Sahzad, A, Kashif, A, Hina, B. Interaction of micropolar fluid structure with the porous media in the flow due to rotating cone. *Alexndria Engineering Journal*. (2021): 60, 1249-1257.
- [20] Cheng, CY. Soret and dufour effects on natural convection boundary layer flow over a vertical cone in a porous medium with constant wall heat and mass fluxes. *International Communications in Heat and Mass Transfer*. (2011a): 38, 44-48.
- [21] Eswaramoorthi, S, Bhuvaneshwari, M, Sivasankaran, S, Rajan, S. Soret and Dufour effects on viscoelastic boundary layer flow over a stretching surface with convective boundary condition with radiation and chemical reaction. *Scientia Iranica, Transactions B: mechanical Engineering*. (2016): 23, 2575-2586.
- [22] Sulonocha, C, Samrat, SP, Sandeep, N. Numerical investigation of magneto-hydrodynamic (mhd) radiative flow over a rotating cone in the presence of soret and chemical reaction. *Propulsion and Power Research*. (2018): 7, 91-101.
- [23] Krishnandan, V, Debozani, B, Sharma, BR. Soret and Dufor effects on MHD flow about a rotating vertical cone in the presence of radiation. *Journal of Maths Comp. Sci.*(2021): 11(3), 3188-3204.
- [24] Hayat, T, Muhammad, T, Al-Mezal, S, Liao, SJ. Forchheimer flow with variable thermal conductivity and cattaneo-christov heat flux. *International Journal of Numerical Methods Heat Fluid Flow*. (2016): 26, 2355-2369.
- [25] Hayat, T, Haider, F, Muhammad, T, Asaed, A. Darcy-Forchheimer flow due to a curved stretching surface with cattaneo-christov double diffusion. *A numerical study. Results Physics*. (2017): 7, 2663-2670.

- [26] Upreti, H, Pandey, AK, Kumar, M. Makinde, OD. Ohmic heating and a non-uniform source/sink roles on 3D Darcy-Forchheimer flow of CNTs nanofluid over a stretching surface. *Arab Journal of Science Engineering*. (2020): 45, 7705-7717.
- [27] Sohail, AK, Hayat, T, Alsaedi, A. Irreversibility analysis in Darcy-Forchheimer flow of viscous fluid with Dufour and Soret effects via finite difference method. *Case Studies in Thermal Engineering*. (2021)26, 101065.
- [28] Loganathan, K, Nazek, A, Fehaid, A, Salem, A. Significances of Darcy-Forchheimer porous medium in third grade nanofluid with entropy features. *European Physical Journal Special Topics*. (2012): 230, 1293-1305.
- [29] Eswaramoorthi, S, Loganathan, K, Muhammad, F, Thongchai, B, Nehad, AS. Analytical and numerical investigation of darcy-forchheimer flow of a nonlinear radiative non newtonian fluid over a riga plate with entropy optimization. *Ain Shams Engineering Journal*. (2023):14, 101887.
- [30] Elsayed, ME, Nasser, SE. Chebyshev finite difference method for effects of variable viscosity and variable thermal conductivity on heat transfer from moving surfaces with radiation. *International Journal of Thermal Science*. (2004): 43, 889-8899.
- [31] Sharma, PR, Singh, G: Effect of variable thermal conductivity and heat source/sink on MHD flow near stagnation point on linear stretching sheet. *Journal of Applied Fluid Mechanics* 2(1) pp 13-21(2009).
- [33]Uwanta, IJ, Usman, H. Effect of variable thermal conductivity on heat and mass transfer flow over a vertical channel with magnetic field intensity. *Applied and Computational Mathematics*. (2014): 3(2) pp 48-56 doi; 10.11648/j.acm.20140302.12.
- [34] Bhuvanavijaya, R, Mallikarjuna. B. Effect of variable thermal conductivity on convective heat and mass transfer over a vertical plate in a rotating system with variable porosity regime. *Journal Architecture and Marine Engineering*. (2014): Doi.org/10.3329/jname.VIII.16488
- [35] Mondal, RK, Abdul-Kalam, MA, Arifuzzaman, SM, Hossain, KE, Ahmed, SF. Unsteady free convective flow along a vertical porous plate with variable viscosity and thermal conductivity. *IOSR Journal of Mathematics*. 2016: 12(4) pp 64-71 .
- [36] Ravichandra Babu, SR, Venkateswatu S, Jaya, LK: Effect of variable viscosity and thermal conductivity on heat and mass transfer flow of nano fluid over a vertical cone with chemical reaction. *International Journal of Applied Engineering Research*. 2018: 13(18) pp 13989-14002.
- [37] Muhammad, A, Sarah, F. A new shooting type method for nonlinear boundary value problems. *Alexandria Engineering Journal*. 2013: 52, 801-805.
- [38] Badradeen, A, Mohsin, HA, H. Shooting method in solving boundary value problems. *International Journal Recent Research and Applied Studies*. 2014: 21(1), 8-30.
- [39] Summiya, P. Numerical solution of the falknerskan equation by using shooting techniques. *IOSR Journal of Mathematics*.(IOSR-JM). 2014: (10)6, 78-83.

[40] Chang, SH. Numerical solution of troesch's problem by simple shooting method. Applied Mathematics and Computation. 2010: 216, 3303-3306.

[41] Uwanta, IJ, Yale, ID, Ahmed, A. Mathematical modelling of steady two dimension MHD fluid flow in a rotating vertical cone in the presence of forchheimer, sores and dufour through a porous medium. International Journal of Science and Applied Research. 2023: 10(2), 14-35.

ABBREVIATIONS

x = Distance along the surface.

y = Distance along the circumferential

z = Distance normal to the surface

r = Radius of the cone

C_p = Specific heat capacity at constant pressure.

h, f, g = Dimensionless velocities.

T = Temperature of the fluid.

L = Cone slant height.

C = Concentration of the fluid.

D = Molecular diffusivity.

D_T = Thermophoresis diffusion coefficient.

Pr = Prandtl number

Gr_L = Grashof number

M = Magnetic field parameter

Da^{-1} = Inverse of Darcy number

θ_0 = Initial temperature of the fluid

B_0 = Magnetic induction parameter

R = Thermal radiation parameter

Cf_x = Skin friction coefficient in x direction

Cf_y = Skin friction coefficient in y direction

Nu_x = Local Nusselt number

Sh_x = Local Sherwood number

Re_L = Reynolds number

Ha^2 = Hartmann number

Pr = Prandtl number

σ_0 = Stefan-Boltzmann constant

k = Absorption coefficient

k_0 = Coefficient of thermal expansion

β_C = Coefficient of concentration expansion

K = Constant permeability of the porous medium
 g = Acceleration due to gravity
 N = Buoyancy ratio
 Sc = Schmidt number
 Sr = Soret number
 k_0 = Effective thermal conductivity
 F_U = Forchheimer
 Df = Dufour
 Q = Variable thermal conductivity parameter

Greek symbols

η = Similarity variable.
 Ω = Angular velocity.
 θ = Dimensionless temperature of the fluid
 λ = Buoyancy parameter
 γ = Chemical reaction parameter
 α = Thermal diffusivity
 ε = Porosity parameter
 σ = Electrical conductivity.
 β_r = Volumetric thermal expansion.
 ρ = Density of the fluid.
 ν = Kinematic viscosity.
 μ = Dynamic viscosity.
 ϕ = Dimensionless concentration.

Subscripts

f = Fluid.
 w = Condition at the wall.
 ∞ = Condition at the free stream.